High-Density Microwave Encoders for Motion Control and Near-Field Chipless-RFID

Cristian Herrojo, *Member, IEEE*, Francisco Muela, Javier Mata-Contreras, Ferran Paredes, *Member, IEEE*, and Ferran Martín, *Fellow, IEEE*

***Abstract*— A novel microwave system for measuring linear displacements and velocities with sub-millimeter resolution and for the implementation of near-field chipless radiofrequency identification (chipless-RFID) systems with very high data capacity is presented. The system is based on a reader, consisting of a half-wavelength straight resonator coupled (through capacitor gaps) to a pair of access lines, and a microwave encoder, in relative motion to the reader and consisting of a linear chain of strips orthogonally oriented to the chain axis. By displacing the encoder over the half-wavelength resonator of the reader, with the encoder strips parallel oriented to the reader axis, the relative velocity and position between the encoder and the reader can be inferred. For that purpose, the reader is fed by a harmonic signal tuned to the resonance frequency that results when an encoder strip is perfectly aligned with the reader. Encoder motion amplitude modulates the feeding signal at the output port, and both the position and the velocity are measured from the peaks, or dips, of the resulting envelope function. Moreover, by making certain strips inoperative, the system can be used for coding purposes. Due to the small period of the encoder (0.6 mm), a high per-unit-length data density in these near-field chipless-RFID tags (i.e., 16.66 bits/cm) is achieved. To illustrate the functionality and potential of the approach, 100-bit chipless-RFID tags with various ID codes are implemented and read.**

***Index Terms*— Displacement sensors, velocity sensors, chipless-RFID, microwave encoders, motion control.**

I. Introduction

There are several approaches for the implementation of displacement and velocity sensors based on microwave technologies. In particular, a significant research effort has been dedicated in the last decade to the development of sensing systems where a transmission line is loaded with resonant elements in relative motion respect to it [1]-[10] (other sensors based on resonator-loaded lines, useful for dielectric characterization and related applications, have been also reported [11]-[25]). In several of the previous spatial sensors, the relative displacement is determined from the variation in the resonance frequency that results when the transmission line and the resonant element are in relative motion (either linear or angular) [2],[6]. In other displacement and velocity sensors, the working principle is coupling modulation [3]-[5],[7]. Although frequency variation and coupling modulation sensors are simple from a technological viewpoint, their resolution and dynamic range are typically limited. Moreover, frequency variation sensors may be subjected to cross sensitivities caused by environmental factors (e.g., frequency drifts caused by temperature variations or changes in ambient moisture), and coupling modulation sensors are very sensitive to noise.

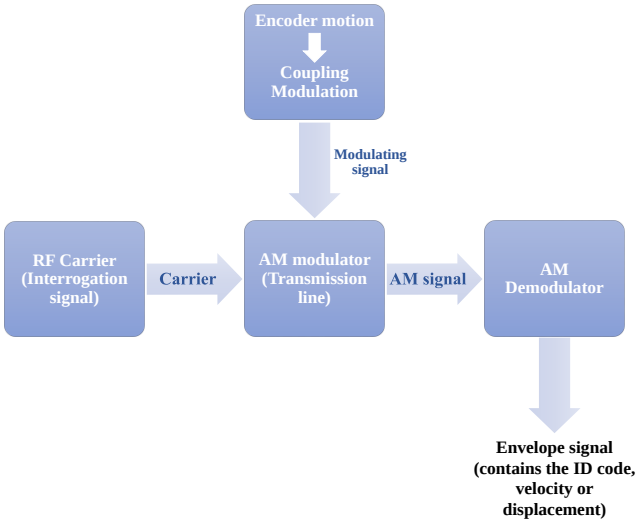

Fig. 1. General block diagram of the AM system used for measuring angular or linear velocities and displacements, or for the implementation of near-field chipless-RFID systems.

In [8], inspired by the optical encoders, a novel approach for the measurement of angular displacements and velocities based on microwaves was proposed. The working principle in such sensors, similar to optical encoders, was pulse detection. However, rather than apertures, which provide the relative displacement and velocity between the moving object and a fixed optical beam used to illuminate the apertures in an optical system, in the sensor reported in [8] the pulses were generated from a chain of resonant elements, particularly split ring resonators [26]. In [8] and in subsequent works [9],[10], such resonator chain was etched in the edge of the rotor, and as many pulses per revolution as resonant elements in the chain (or twice this value) were achieved. Up to 1.200 pulses,

This work was supported by MINECO-Spain (projects TEC2016-75650-R and RTC-2017-6303-7), Generalitat de Catalunya (project 2017SGR-1159), ICREA, and by FEDER funds. C. Herrojo acknowledges MINECO for supporting his research activity through the FPI grant BES-2014-068164.

C. Herrojo, F. Muela, F. Paredes and F. Martín are with GEMMA/CIMITEC, Departament d'Enginyeria Electrònica, Universitat Autònoma de Barcelona, 08193 Bellaterra, Spain. E-mail: Ferran.Martin@uab.es.

J. Mata-Contreras is with the Departamento de Ingeniería de Comunicaciones, Escuela Técnica Superior de Ingeniería de Telecomunicación, Universidad de Málaga, 29071 Málaga, Spain.

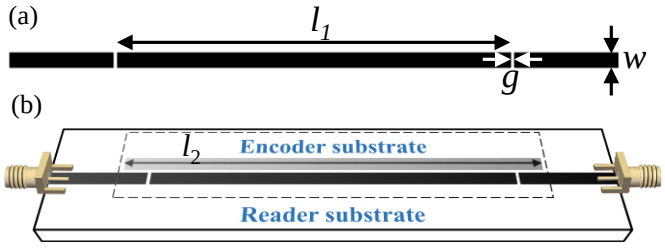

Fig. 2. Layout of the reader (a), and three-dimensional view of the reader with a strip on top of it and perfectly aligned (b). Dimensions are (in mm): l_1= 21.2, l_2= 22.4, g = 0.2 and w = 0.4. The considered reader substrate is the *Rogers RO4003C* with dielectric constant ε_r = 3.55, thickness h = 0.81 mm and loss tangent tanδ = 0.0021. The considered encoder substrate is the *Rogers RO4003C* with dielectric constant ε_r = 3.55, thickness h = 0.204 mm and loss tangent tanδ = 0.0021.

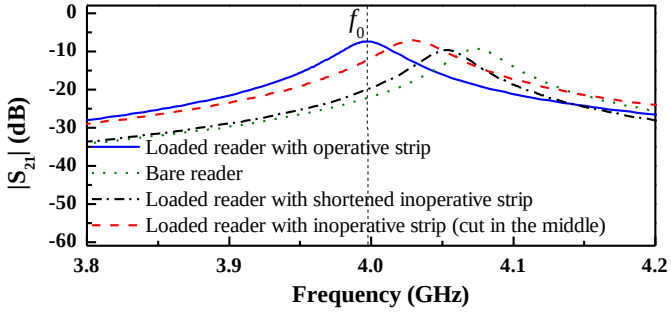

Fig. 3. Simulated frequency responses (including losses) of the bare reader, and reader loaded with perfectly aligned strips under different conditions, including operative strip with nominal length, inoperative strip with cut in the middle position, and inoperative strip with shortened length. The considered air gap, or vertical distance between the tag and the reader is 0.2 mm. In all the simulations a pair of adjacent operative strips has been considered.

providing an angular resolution of 0.3º, were demonstrated in [9]). For pulse generation, caused by rotor motion, a transmission line conveniently designed, acting as the stator of the sensor system, was used in [8]-[10]. Through tag motion, line-to-resonator coupling is modulated, and consequently the transmission coefficient is modulated as well. Therefore, by feeding the line with a harmonic signal conveniently tuned (i.e., in the vicinity of the resonance frequency of the resonant elements), the output signal is amplitude modulated (AM), and the time distance between adjacent pulses, or dips, in the envelope function is related to the relative velocity between the stator and the rotor (Fig. 1). Therefore, relative instantaneous velocities as well as displacements between the stator and the rotor can be measured. Like in optical systems, a figure of merit in these velocity and displacement sensors is the number of pulses per time unit, intimately related to the number of resonant elements per unit length. Thus, to increase the number of pulses, it is necessary to reduce the period of the resonator chain as much as possible.

The main aim of this paper is to implement a linear displacement and velocity sensor based on coupling modulation, similar to those reported in [8]-[10] for angular measurements, with a period significantly smaller. For this purpose, a novel reader and chain are designed. To optimize the chain period, very narrow (0.4 mm) and tiny separated (0.2 mm) linear strips, oriented in the direction orthogonal to the chain axis, are considered. By this means, we achieve a very high density of strips per unit length, providing a high number of pulses per time unit (obviously, the time density of pulses is also determined by the relative velocity between the chain and the reader). Moreover, as long as we can force the strip chain to contain some inoperative strips, i.e., strips not detectable as pulses by the reader, we can use this system for coding purposes. Within this scenario, each strip provides a bit of information with the logic state set to '1' or '0' depending on whether the corresponding strip is operative or not. The strip chain containing the code can be read through near-field by means of the same reader used for measuring the linear displacement or velocity. In this case, however, only the pulses of those bits set to '1' will appear in the envelope function. Since these chipless-RFID tags are implemented as chain patterns, reducing the chain period (as it is demonstrated in this paper) is fundamental in order to implement high data capacity systems compatible with short tags (the 100-bit tags reported in this paper are significantly shorter than other previous tags with lower number of bits, used in similar near-field chipless-RFID systems [27]-[34]).

II. Working Principle and Design

The principle of the proposed sensor and chipless-RFID system is based on the variation of the transmission coefficient of a bandpass microstrip structure (particularly an order-1 capacitively-coupled half-wavelength resonator bandpass filter) experienced when a straight metallic strip, etched in an independent substrate, is located on top of it at short distance. Thus, in the proposed sensing/chipless-RFID system the active part of the reader is a capacitively-coupled half-wavelength resonator bandpass filter fed by a harmonic signal [see Fig. 2(a)]. The transmission coefficient of the bare structure, i.e., without strip on top of it (but with the presence of the substrate where the strips are etched), exhibits a resonance peak at roughly the frequency where the length of the line is equivalent to a half wavelength. Actually such frequency depends also on the pair of gaps present between the central line section and the input and output access lines, since such gaps provide a non-negligible reflection phase due to its capacitive effect. The resonance condition can be written as

$$\varphi_1 + \varphi_2 + 2\beta l_1 = 2\pi n \qquad (1)$$

where φ_1 and φ_2 are the reflection phases in gaps 1 and 2, respectively, βl_1 is the electrical length of the central transmission line section, β and l_1 being the phase constant and the physical length of such section, and n = 1, 2, 3,.... From (1), it follows that for an uncoupled resonator (with φ_1 = φ_2 = 0), the first resonance (n = 1) occurs when $\beta l_1 = \pi$ (or l_1 = $\lambda/2$, where λ is the guided wavelength), as it is well known.

From (1), it is clear that the resonance condition can be altered either by modifying the reflection phases or by perturbing the phase constant (or both simultaneously). This can be achieved by the presence of a straight strip on top of the half-wavelength resonator, parallel oriented to the line axis, with a length extending over the gap positions, as indicated in Fig. 2(b). Figure 3 depicts the response of the bare

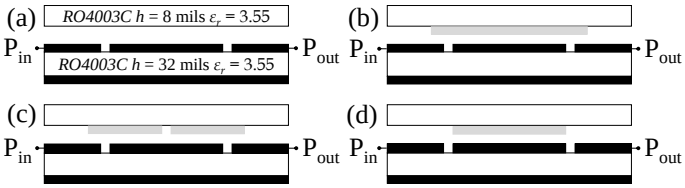

Fig. 4. Cross-sectional view of the strips and reader corresponding to the four responses depicted in Fig. 3. (a) Bare reader; (b) loaded reader with operative strip; (c) loaded reader with inoperative strip with a cut in the central position; (d) loaded reader with shortened inoperative strip.

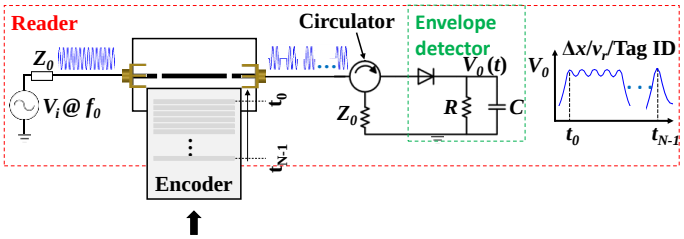

Fig. 5. Sketch illustrating the operation principle of the displacement/velocity sensor and chipless-RFID system.

reader inferred from full wave electromagnetic simulation (using *Keysight Momentum*), as well as the response of the reader with a perfectly aligned strip on top of it, where it can be appreciated that the resonance peak is shifted to lower frequencies. Actually, the responses of the bare and loaded reader have been obtained by considering the presence of adjacent strips separated 0.2 mm (corresponding to a period of 0.6 mm). The reason is that for the measurement of displacements and velocities, a strip chain is necessary, as will be later shown.

For the application of this structure (reader and strip chain) to near-field chipless-RFID, it is necessary to make inoperative those strips of the tag corresponding to the logic state '0'. The most canonical option is to eliminate such strips (so that bit encoding is determined by the presence or absence of strip). However, this is not the best option, in terms of cost, for massive tag manufacturing, since each code needs a different mask. Therefore, the preferred strategy in a real scenario is to fabricate all-identical tags (using massive printing processes such as screen-printing, rotogravure, flexography, etc.), and then personalize (program) the tags by means of low-cost systems, such as inkjet or laser ablation.

In [31]-[34], tag programming was achieved by cutting certain resonant elements in the tag chain (making them inoperative). In the system presented in this work, we have considered two options to "write" the logic '0' (strip inoperative). The first one is to cut the strip in the central position [see Fig. 4(c)]. The transmission coefficient, also depicted in Fig. 3, is different to the one corresponding to the presence of a functional strip on top of the reader, but it is far from the response of the bare reader. The reason is thought to be due to the fact that the main cause of resonance variation is the modification of the effective capacitance of the gap, which is not altered by implementing a cut in the central position of the strip. The second approach consists of shortening the strips by the extremes [see Fig. 4(d)], providing a strip length

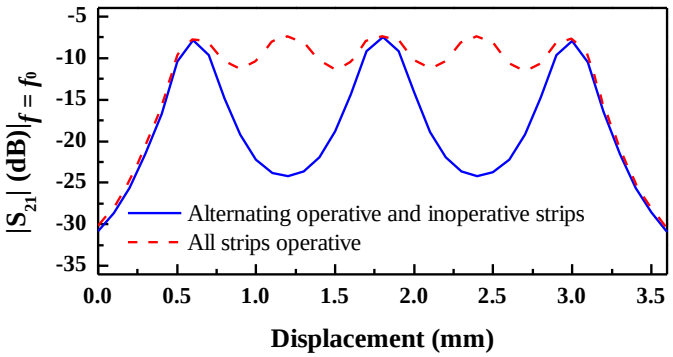

Fig. 6. Transmission coefficient at f_0 as a function of the relative displacement between the reader and the strip chain. Two cases are considered, i.e., with all strips operative, and with operative and inoperative (shortened) strips alternating.

identical to the one of the resonant element of the reader. By this means, the effect of the strip on the gap capacitance is expected to be smaller, and, consequently, a response closer to the one of the bare reader is expected. This is confirmed in Fig. 3, where such response is also depicted. According to these results, tag programming should be done through the second considered approach, i.e., by shortening the strip, since the resulting response, very similar to the one of the bare reader, exhibits a significant excursion of the transmission coefficient at the resonance frequency of the reader loaded with operative strip, f_0, indicated in Fig. 3.

For the measurement of displacements and velocities, as well as for tag reading in a near-field chipless-RFID scenario, the idea is to displace the strip chain above the reader at short distance (the considered air gap in the results depicted in Fig. 3 is 0.2 mm). For proper tag reading or displacement/velocity measurement, it is necessary that the strip chain is oriented with the strips parallel to the reader axis. Moreover, the central position of the strips must coincide to a good approximation with the central position of the half-wavelength resonator of the reader. By tuning the feeding harmonic signal of the reader to f_0 (the resonance peak of the loaded reader), the amplitude of the output signal is expected to be modulated by strip (or tag) motion. From the envelope function, which can be inferred from an envelope detector preceded by an isolator (to avoid unwanted reflections from the diode), the relative velocity/displacement between the strip chain in motion and the fixed reader, or the identification (ID) code of the tag, can be inferred. The operation principle is illustrated in Fig. 5.

For displacement and velocity measurements, all the strips should be present and functional for resolution optimization. Since the chain period is known (0.6 mm in our case), from the distance between adjacent peaks, or dips, in the envelope function, the velocity of the strip chain in motion can be obtained. The relative displacement can be simply derived from the number of cumulative peaks, or dips, appearing from a reference position. According to Fig. 3, the excursion experienced by the transmission coefficient at f_0 when the strip is made inoperative (by shortening it) is significant. However, this does not ensure an important variation of the transmission coefficient at that frequency by strip motion, if the strips are

tiny separated (as pursued in this work for resolution optimization). To analyze this important aspect, we have obtained the transmission coefficient at f_0 for different relative displacements between the reader and the strip chain (where 5 operative strips separated 0.2 mm, providing a chain period of 0.6 mm, have been considered). The result is depicted in Fig. 6. It can be seen that the variation of the transmission coefficient is roughly 3.7 dB, which may be enough to achieve a non-negligible modulation index in the output signal of the reader line, and hence an envelope function with readable (distinguishable) peaks, or dips.

By alternating the functionality of the strips (i.e., the central and the outer strips operative and the other two shortened), roughly equivalent to duplicate the chain period, the excursion experienced by the transmission coefficient is as high as 16.4 dB (see Fig. 6). This later situation is much better in terms of robustness, since a larger dynamic range in the envelope function is expected, but with the penalty of a degraded resolution. For this main reason, we have maintained the period of the strip chain in 0.6 mm in the fabricated chains (or tags). Obviously, intermediate periods can be considered, but, as mentioned, the main aim of this paper is to drive the resolution to the limits imposed by the available technology (the period in the resonant chains of the sensors reported in [9],[10], based on a similar principle, is 2.2 mm).

This small resolution for displacement and velocity measurements has direct impact on data density when the structure is used as chipless-RFID system. In this later case, the relative velocity between the reader and the tag (the strip chain) must be well known and stable during a reading operation. From a mechanical viewpoint, implementing a guiding system providing a uniform tag speed in a real scenario is not an issue (nevertheless, this mechanical aspect is out of the scope of this paper, purely focused on the electromagnetic and electronic blocks of the system). The need to know the tag velocity with regard to the reader comes from the fact that such velocity determines the time instants where the envelope function must be read. In this regard, it should be mentioned that header bits with all strips operative ('1') may be added at the beginning of the ID code in order to provide the information relative to the tag velocity.

Another important aspect related to robustness, is the readability of the system when it is subjected to mechanical vibrations or misalignments. Thus, we have studied the effects of misalignment/orientation and vertical distance (gap) variation between the reader and the strip chain on the response of the system, particularly, the transmission coefficient at f_0. For that purpose, a case example has been considered, i.e., a 5-strip chain with alternating operative and inoperative strips (identical to the one considered in Fig. 6). Figure 7(a) depicts the simulated responses obtained by displacing the strip chain over the reader for different lateral misalignments. It can be seen that the system is tolerant up to lateral displacements of roughly ±0.8 mm (above that value, the operative and inoperative strips cannot be distinguished). Nevertheless, it should be mentioned that by elongating the strips (with the penalty of larger size), the above tolerance in lateral displacement can be improved.

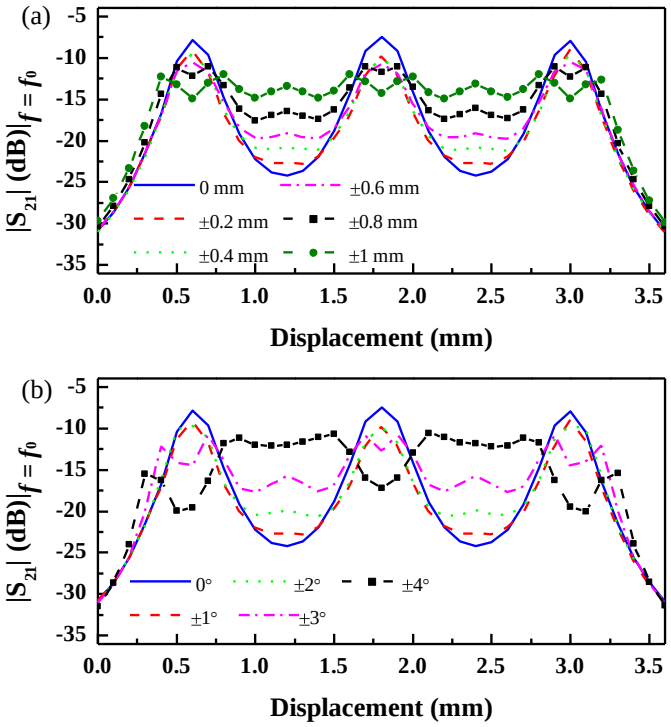

Fig. 7. Effects of lateral misalignment (a) and lack of alignment by rotation (b) on the transmission coefficient at f_0 when the strip chain is displaced over the reader. The considered air gap is 0.2 mm.

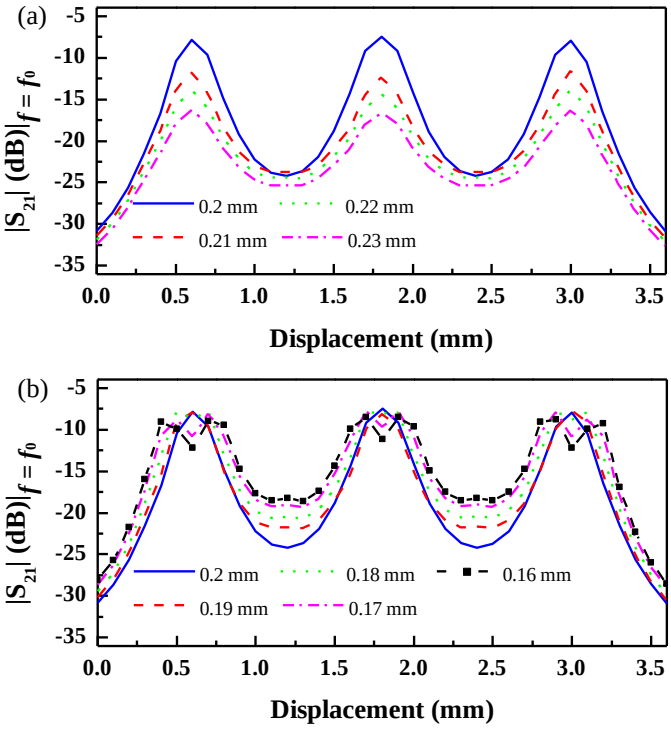

Fig. 8. Effects of air gap on the transmission coefficient at f_0 when the strip chain is displaced over the reader. (a) Air gaps above 0.2 mm; (b) air gaps below 0.2 mm.

Let us now consider the effects of misalignment in relative orientation (rotation) between the strip chain and the reader.

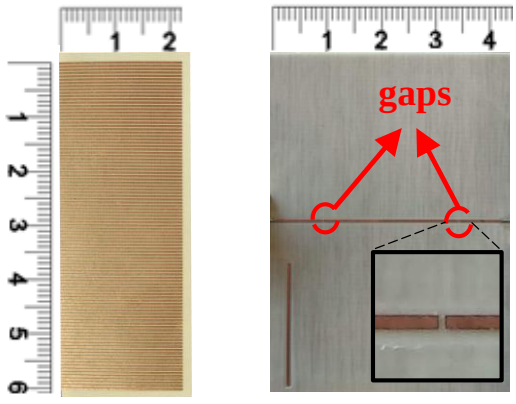

(a) (b)

Fig. 9. Photograph of the strip chain (a) and active part of the reader (b).

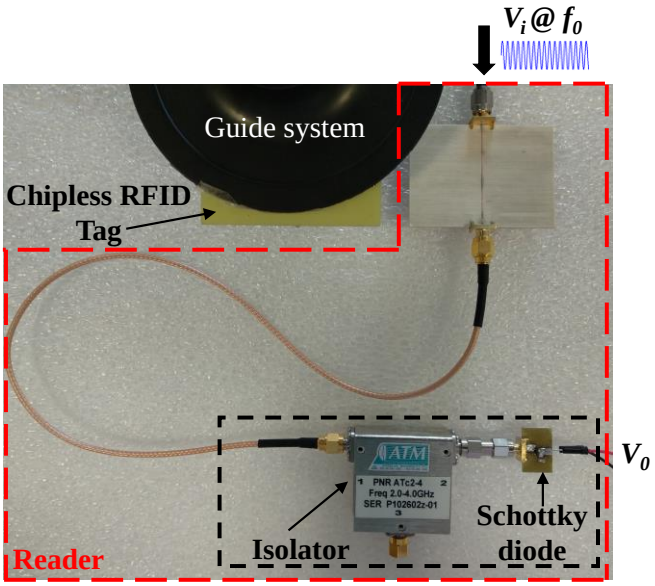

Fig. 10. Photograph of the experimental setup.

For that purpose, we have obtained the response inferred by displacing the strip chain over the reader for different angles between the line axis (reader) and the axis of the strips in the chain (the perfect situation corresponding to an angle of 0º). The results, depicted in Fig. 7(b), indicate that the system is tolerant up to an angle of roughly ±3º, which is reasonable from a practical viewpoint. Better tolerance against lack of alignment by rotation can be obtained, but at the expense of wider line and strips (which represents a penalty in terms of data density for chipless-RFID systems and resolution for linear displacement measurements).

The effects of the air gap on the response of the system can be seen in Fig. 8. The structure has been optimized for a nominal air gap of 0.2 mm, where the maximum excursion of the transmission coefficient results. Increasing the air gap [Fig. 8(a)] reduces such excursion, but reasonable values are obtained within the considered margin (up to 0.23 mm). Figure 8(b) shows the responses that have been inferred by decreasing the air gap. It is shown that even for a vertical distance between the strip chain and the reader as small as 0.16 mm, the excursion experienced by the transmission coefficient is reasonable. Hence, according to these results, we can conclude that system tolerance against vertical distance is at least in the range 0.16-0.23 mm.

It is worth mentioning that for air gaps of 0.16 mm and 0.17 mm, a double peak in the response is visible. This is due to the fact that by decreasing the air gap, the maximum in the frequency response of the structure (coincident with f_0 in Fig. 3, where the air gap is 0.2 mm) is displaced to the left. Under these conditions, two separated maxima are expected when the strip chain is displaced above the reader and the frequency of the injected signal is f_0. Obviously, such maxima are visible (double peak) when the frequency of the maximum transmission coefficient lies significantly below f_0, and this occurs for sufficiently small air gaps (such as 0.16 mm and 0.17 mm in our case).

III. Experimental Results and Discussion

a. Linear displacement and velocity sensor

We have fabricated a strip chain consisting of 100 all-identical operative strips by means of photo-etching on the substrate indicated in the caption of Fig. 2. The active part of the reader (i.e., the capacitively coupled half-wavelength resonator bandpass filter) has been fabricated by means of a milling machine *LPKF-H100* on the substrate also indicated in the caption of Fig. 2. The photographs of the chain and reader are depicted in Fig. 9.

The frequency of the feeding (carrier) signal has been set to f_0 = 4 GHz, and such signal has been generated by means of the function generator *Agilent E4438C*. The envelope function of the AM modulated signal present at the output port of the active part of the reader has been inferred by means of an envelope detector implemented by means of the *Avago HSMS-2860* Schottky diode and the *N2795A* active probe (with capacitance 1 pF and resistance 1 MΩ). Such envelope detector has been preceded by an isolator (implemented by means of a circulator, model *ATM ATc4-8*), in order to avoid mismatching reflections from the diode, a highly nonlinear device. The displacement of the strip chain over the active part of the reader has been achieved by means of an in-house guiding system to which the chain has been attached. The photograph of the experimental setup is shown in Fig. 10.

After adequately orienting and positioning the strip chain over the reference position, we have displaced the chain, and we have recorded the envelope function in an oscilloscope (model *Agilent MSO-X-3104A*). The resulting envelope function is depicted in Fig. 11. Note that this function is not exactly periodic. This is mainly due to the non-uniformity of the air gap during the displacement of the strip (note also that our guiding system cannot guarantee a uniform velocity, as well). Nevertheless, from the distance between adjacent peaks, or dips, the instantaneous linear velocity can be obtained. According to the figure, the dips (appearing when the intermediate position between two strips is perfectly aligned with the line axis of the reader) are clearly visible and easily identifiable. Such dip times, which can be easily recorded by means of a post-processing unit, are then used to determine the

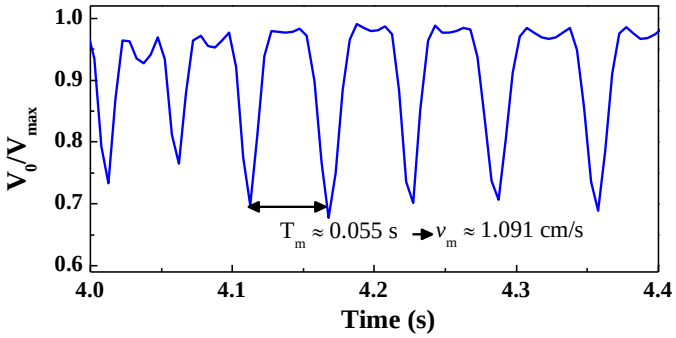

Fig. 11. Measured normalized envelope function obtained by displacing the strip chain over the reader (only a portion of the curve is shown for a better view).

linear velocity and the relative displacement between the reader and the chain from the reference position. According to Fig. 11, the average time interval between adjacent dips is 0.055 s, corresponding to an average displacement velocity of 1.09 cm/s.

The main advantage of this system for the measurement of linear displacements and velocities is the fact that it exhibits a large input dynamic range and, simultaneously, very good resolution. Particularly, the resolution for linear displacement measurement is dictated by the period, which is only 0.6 mm. This is a very small resolution if we take into account that the input dynamic range is only limited by the total length of the strip chain. Therefore, this system may be of interest for motion control, in applications where sub-millimeter resolution and dynamic ranges of several centimeters or even meters are needed. In displacement sensors based on a transmission line loaded with a single resonant element (e.g., those reported in [2]-[6]) the resolution can be driven to lower values, but the dynamic range is roughly limited by the size of the resonant element, i.e., far from the dynamic ranges achievable with the approach reported in this work.

For the measurement of instantaneous velocities, the key figure of merit is the number of pulses per time unit, dictated by the period of the strip chain (and obviously by the motion speed). In this work, we have achieved a substantially smaller period than those of other previously reported displacement and velocity sensors [9],[10] (applied to the measurement of angular velocities). This has been achieved by simply replacing the rectangular resonant elements of the chains used in [9],[10] by straight strips (orthogonally oriented to the chain axis), and, obviously, by designing a new reader, able to detect the functionality, or not, of such strips. By this means, the period has been reduced from 2.2 mm in [9],[10] to 0.6 mm in the sensor reported in this work.

Note that the variation experienced by the envelope function in Fig. 11 reasonably correlates with the variation of the transmission coefficient in Fig. 6. According to this figure, the difference between the minima and the maxima of the transmission coefficient at f_0 (when all the strips are operative) is roughly −3.7 dB, which corresponds to a power ratio of 0.42 and to a voltage ratio of 0.65, close to the ratio between the dip and peak levels in Fig. 11. This is a relatively high ratio

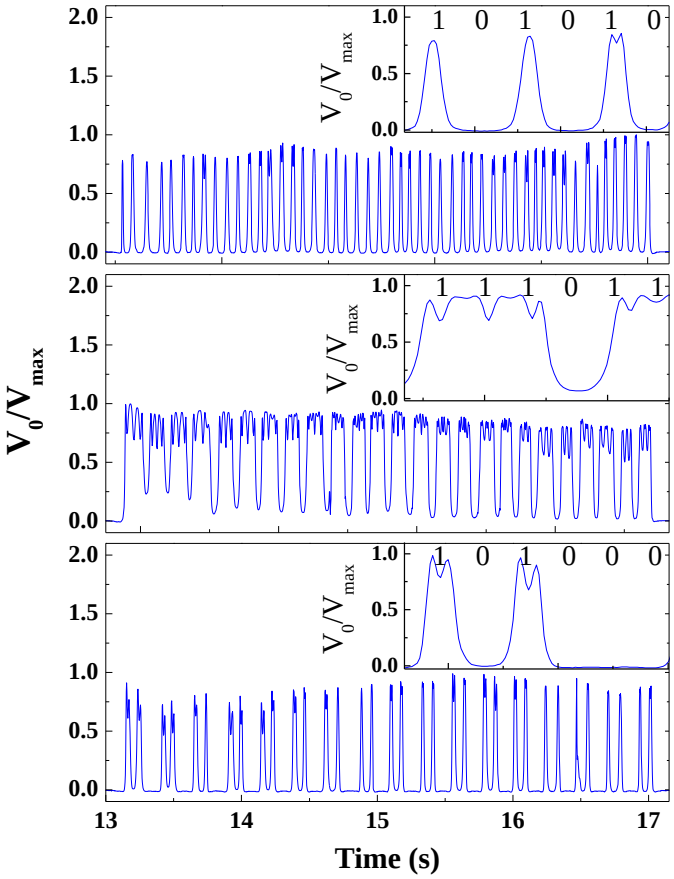

Fig. 12. Measured normalized envelope function corresponding to the tags with the indicated codes (shown in the insets, where zoom views are included for clarity).

(although the peaks and dips can be perfectly discerned), which is due to the fact that the resolution has been driven to the limits, as discussed before. Note that by increasing somehow the period of the strip chain, yet preserving a good resolution, the ratio between the dip and peak levels in the envelope function is expected to be significantly improved (reduced). Note, for instance, that with a period of 1.2 mm (equivalent to alternating operative and inoperative strips in a 0.6mm-period chain), the variation in the transmission coefficient is as large as 16.4 dB (see Fig. 6). Consequently, a smaller ratio between the dip and peak levels in the envelope function should be expected in this case.

Concerning the maximum velocity that can be measured with the proposed system, in a real scenario it is dictated by the sampling frequency of the acquisition system, f_s. For reasonable values of f_s, extremely high velocities can be measured. For instance, if we consider a minimum number of samples per cycle of the envelope function (distance between adjacent pulses or dips) and this number is set to 100 samples per cycle, then it follows that the time period (distance between adjacent pulses, t_p) should be not less than $100/f_s$, i.e., $t_p > 100/f_s$. Therefore, the velocity must satisfy $v_p < p/t_p$, where p is the period of the encoder (p = 0.6 mm in our case), and the maximum velocity that can be measured, by considering a reasonable sampling frequency of f_s = 100 MHz, is found to be 600 m/s, which is more than enough for most

applications. Concerning the lower limit, velocities as small as required can be measured, obviously, assuming that at least two adjacent pulses (or dips) are needed to determine the relative velocity between the tag and the reader.

With regard to velocity resolution, it is related to time resolution, given by the inverse of the sampling frequency (i.e., $t_{res} = 1/f_s$). Since the velocity can be expressed as

$$v_p = \frac{p}{T_m \pm t_{res}} \approx \frac{p}{T_m}\left(1 \mp \frac{t_{res}}{T_m}\right), \quad (2)$$

T_m being the time distance between adjacent pulses, it follows that the velocity resolution is given by

$$v_{p,res} = \frac{p t_{res}}{T_m^2} = v_p \frac{t_{res}}{T_m} = v_p^2 \frac{t_{res}}{p} \quad (3)$$

and it depends on the linear velocity. To give an idea of specific values, the velocity resolution resulting from (3), by considering a nominal velocity of 0.1 m/s (with p = 0.6 mm and f_s = 100 MHz), is as small as 1.66×10^{-7} m/s. By considering a higher velocity, e.g., 100 m/s, the resolution is found to be 0.166 m/s. Note that for a given period and sampling frequency, or t_{res}, the resolution varies quadratically with the nominal velocity. This explains the degradation of the resolution with velocity. Indeed, a relevant parameter is the ratio between the resolution and velocity, i.e.,

$$\frac{v_{p,res}}{v_p} = v_p \frac{t_{res}}{p} \quad (4)$$

which is found to be proportional to the nominal velocity.

Another important parameter related to sensor performance is the error in the determination of the linear velocity. As long as the time period in this work is determined from the distance between adjacent dips (see Fig. 11), such error depends on dip width and distance between dips. As it was pointed out in [9],[10], narrower dips provide smaller error. Nevertheless, the accuracy can be improved either by averaging over several dips, or by considering distant dips (assuming in both cases a degradation in the ability of the sensor to detect velocity variations in small time lapses). Dip width can be estimated by a predefined percentage variation from the minima, e.g., 2%. With this (conservative) value, the ratio between the dip width and distance between adjacent dips is found to be 0.03, corresponding to a time error of 3% and roughly to the same velocity error. Note, however, that such error can be reduced by an order of magnitude by simply determining the velocity from the time interval corresponding to 10 dips.

b. Chipless-RFID system

To demonstrate the potential of this system for near field-chipless-RFID applications, we have programmed three codes from the single fabricated 100-bit tag with all bits set to '1', i.e., the strip chain shown in Fig. 9(a). As mentioned before, the different codes have been generated by slightly shortening those strips associated to the logic state '0'. We have done this by a milling procedure, but processes such as laser ablation can be envisaged in a real scenario. Alternatively, all-identical tags with all bits set to '0' (i.e., with shortened strips) can be fabricated, and then programmed by elongating the metallization of certain strips (those which should be set to '1') by means of a printing process (e.g., inkjet printing). The normalized envelope functions and the generated codes are depicted in Fig. 12. It can be seen that the tags are correctly read by virtue of the maxima and minima associated to the logic '1' and '0' states, respectively. Note that in the tag with sequence '101010…' the average ratio between the minimum and the maximum in the envelope function is very small, in agreement with the 16.4 dB variation in the transmission coefficient at f_0 inferred by displacing the tag (see Fig. 6). Such envelope function confirms the smaller achievable ratios between dips and peaks when the "effective" chain period is increased, as anticipated before.

Conceptually, the present near-field chipless-RFID system is similar to those reported in previous papers [27]-[34]. However, the main benefit of the proposed system is the fact that the tag period has been substantially reduced. This means that the per-unit length data density, as high as 16.66 bits/cm, is substantially larger than in the tags reported, e.g., in [31]-[33] (specifically, more than 5 times larger). Indeed, the proposed 100-bit tag is as short as 6 cm. By contrast, the 84-bit tag reported in [33] exhibits a length of 26.7 cm (corresponding to a per unit length data density of 3.14 bit/cm). Obviously, by using straight strips orthogonally oriented with regard to the chain axis, the width of the proposed tags (2.24 cm) is larger than the one of the tags reported in [33] (0.35 cm). However, in these tags based on near-field coupling and sequential bit reading, implemented as chains of metallic patterns, the limiting factor (when a large number of bits is necessary) is dictated by tag length, provided the width is constrained within reasonable values. Therefore, the proposed approach represents a good solution in this regard. The data capacity of the presented tags (100 bits) is by far larger than the data capacity reported to date in other chipless-RFID tags (an exhaustive comparative analysis of the different chipless-RFID technologies can be found in [34]).

Another important difference between the present system and those reported in [27]-[34] concerns the fact that in the structures reported in the above references, the tag chain is composed of resonant elements, and such elements are identical to the one present in the reader (either S-shaped split ring resonators, S-SRRs, or simply SRRs). In this paper, the elements of the tag (straight strips) modify the resonance frequency of the reader line (an order-1 bandpass filter), thereby modulating the amplitude of the interrogation signal, but such elements do not act as resonant elements. Note also that the microwave part of the reader, the one needed to detect the presence of operative or inoperative strips through the amplitude of the envelope function, is completely different as compared to papers [27]-[34].

The main focus of this paper has been to decrease the period of the tag chain as much as possible in order to improve the resolution in the displacement sensor, and the density of bits per unit length in the chipless-RFID system. We have achieved a period of 0.6 mm, much smaller than those reported in the chipless-RFID systems of [27]-[34] and in the

angular velocity sensors of [8]-[10]). Such small period has been achieved thanks to the new combination of encoder and reader topology, able to detect the dips/pulses with such small separation between the tag elements. Moreover, although the excursion experienced by the transmission coefficient (as consequence of a bit variation in the ID coding sequence) is larger in [31]-[33], it can be appreciated in Fig. 12 that the different codes can be perfectly read.

It is worth mentioning that a properly encoded tag (e.g., with a non-symmetric periodic sequence) may be used as linear displacements and velocity sensor, with the capability to detect the direction of motion. Note, however, that motion direction detection with this procedure has the penalty of a worst displacement resolution, due to the reduction in the number of pulses. Also, the capability to measure instantaneous velocities is degraded, since variations in time lapses smaller than the encoder period cannot be detected. Nevertheless, in its functionality as linear displacement and velocity sensor, either with all functional resonators or with an encoded sequence, the proposed structure may be useful for many motion control applications, where the velocity does not experience strong variations with time.

IV. Conclusions

In conclusion, a novel near-field approach useful for the measurement of linear displacements and instantaneous velocities, as well as for the implementation of chipless-RFID systems has been presented in this paper. The approach is based on a periodic chain of straight metallic strips etched on a dielectric substrate. Such strips chain acts as the mobile element in the displacement/velocity sensor, or as the element containing the ID code (or tag) in the chipless-RFID system. In this later case, however, certain strips should be slightly shortened (making them inoperative), according to the required bit code, since each strip in the chain corresponds to a single bit element. For tag reading, an element able to distinguish the longer and shorter strips is required, and for that purpose, a capacitively coupled half-wavelength resonator order-1 bandpass filter (the active part of the reader), fed by a harmonic signal conveniently tuned, has been used. Such element has been also used for displacement and velocity measurements, since, with additional electronics, it is able to provide the time interval between two adjacent strips crossing a fixed point (the reader), and hence the relative velocity and displacement. For such measurements, and for tag reading, the strip chain is displaced above the active part of the reader, in close proximity to it. By this means, the output signal is amplitude modulated due to the effects of the operative strips on the transmission coefficient at the frequency of the feeding signal, and the information relative to the displacement and velocity, as well as the ID code, is contained in the envelope function. As sensing element, the reported device exhibits sub-millimeter resolution (0.6 mm) and high input dynamic range for linear displacement measurement. Moreover, by virtue of the small chain period, the number of pulses per unit time, a figure of merit in sensors devoted to the measurement of instantaneous velocities, is very high. The main advantage of the proposed system for chipless-RFID applications is the achievable data capacity (100-bit tags have been reported), compatible with small-sized tags, as short as 6 cm in the present work. This high per unit length data capacity, the most important figure of merit in chipless-RFID tags based on near-field coupling and sequential bit reading, has been achieved, again, thanks to the small period of the designed and fabricated tags. The reported devices may be of interest for accurate control motion, and for chipless-RFID, in applications where the read distance can be sacrificed in favor of a high data capacity (e.g. secure paper). To the best of our knowledge, 100-bit chipless-RFID tags have been never reported to date.

References

[1] M. Schueler, C. Mandel, M. Puentes, and R. Jakoby, "Metamaterial inspired microwave sensors," *IEEE Microw. Mag*., vol. 13, no. 2, pp. 57–68, Mar. 2012.

[2] C. Mandel, B. Kubina, M. Schüßler, and R. Jakoby, "Passive chipless wireless sensor for two-dimensional displacement measurement," Proc. *41st European Microwave Conf*., Manchester, UK, 2011, pp. 79–82.

[3] J. Naqui, M. Durán-Sindreu and F. Martín, "Novel Sensors Based on the Symmetry Properties of Split Ring Resonators (SRRs)", *Sensors*, vol 11, pp. 7545-7553, 2011.

[4] A. Karami-Horestani, C. Fumeaux, S.F. Al-Sarawi, and D. Abbott, "Displacement sensor based on diamond-shaped tapered split ring resonator," *IEEE Sensors J*., vol. 13, no. 4, pp. 1153-1160, Apr. 2013.

[5] A. Horestani, D. Abbott, and C. Fumeaux, "Rotation sensor based on horn-shaped split ring resonator," *IEEE Sens. J*., vol. 13, no. 8, pp. 3014–3015, May 2013.

[6] A. Ebrahimi, W. Withayachumnankul, S. Al-Sarawi, and D. Abbott, "Metamaterial-inspired rotation sensor with wide dynamic range," *IEEE Sensors J*., vol. 14, no. 8, pp. 2609-2614, Aug. 2014.

[7] J. Naqui, and F. Martín, "Angular displacement and velocity sensors based on electric-LC (ELC) loaded microstrip lines", *IEEE Sensors J*., vol. 14(4), pp. 939-940, Apr. 2014.

[8] J. Naqui, F. Martín, "Application of broadside-coupled split ring resonator (BC-SRR) loaded transmission lines to the design of rotary encoders for space applications", *IEEE MTT-S Int. Microw. Symp.* (IMS'16), San Francisco (CA), May 2016.

[9] J. Mata-Contreras, C. Herrojo, and F. Martín, "Application of split ring resonator (SRR) loaded transmission lines to the design of angular displacement and velocity sensors for space applications", *IEEE Trans. Microw. Theory Techn*., vol. 65, no. 11, pp. 4450-4460, Nov. 2017.

[10] J. Mata-Contreras, C. Herrojo, and F. Martín, "Detecting the rotation direction in contactless angular velocity sensors implemented with rotors loaded with multiple chains of split ring resonators (SRRs)", *IEEE Sensors J*., vol.18, no. 17, pp. 7055-7065, Sep. 2018.

[11] M. S. Boybay and O. M. Ramahi, "Material characterization using complementary split-ring resonators," *IEEE Trans. Instrum. Measur*., vol. 61, no. 11, pp. 3039–3046, 2012.

[12] C.-S. Lee and C.-L. Yang, "Complementary split-ring resonators for measuring dielectric constants and loss tangents," *IEEE Microw. Wireless Compon. Lett.*, vol. 24, no. 8, pp. 563−565, Aug. 2014.

[13] C.-L. Yang, C.-S. Lee, K.-W. Chen, and K.-Z. Chen, "Noncontact measurement of complex permittivity and thickness by using planar resonators," *IEEE Trans. Microw. Theory Techn.*, vol. 64, no.1, pp. 247−257, Jan. 2016.

[14] W. Withayachumnankul, K. Jaruwongrungsee, A. Tuantranont, C. Fumeaux, and D. Abbott, "Metamaterial-based microfluidic sensor for dielectric characterization," *Sensor Actuat. A Phys*., vol. 189, pp. 233-237, Jan. 2013.

[15] A. Ebrahimi, W. Withayachumnankul, S. Al-Sarawi, and D. Abbott, "High-sensitivity metamaterial-inspired sensor for microfluidic dielectric characterization," *IEEE Sensors J*., vol. 14, no. 5, pp. 1345-1351, May 2014.

[16] A. Abduljabar, D. Rowe, A. Porch, and D. Barrow, "Novel microwave microfluidic sensor using a microstrip split-ring resonator," *IEEE Trans. Microw. Theory Tech*., vol. 62, no. 3, pp. 679-688, Mar. 2014.

[17] T. Chretiennot, D. Dubuc, and K. Grenier, "A microwave and microfluidic planar resonator for efficient and accurate complex permittivity characterization of aqueous solutions," *IEEE Trans. Microw. Theory Techn*., vol. 61, no. 2, pp. 972–978, Feb. 2013.
[18] A. Ebrahimi, W. Withayachumnankul, S. F. Al-Sarawi and D. Abbott, "Microwave microfluidic sensor for determination of glucose concentration in water," *2015 IEEE 15th Mediterranean Microwave Symposium* (MMS), Lecce, 2015, pp. 1-3.
[19] A. Salim and S. Lim, "Complementary split-ring resonator-loaded microfluidic ethanol chemical sensor," *Sensors*, vol. 16, pp. 1-13, 2016.
[20] P. Vélez, L. Su, K. Grenier, J. Mata-Contreras, D. Dubuc, and F. Martín, "Microwave microfluidic sensor based on a microstrip splitter/combiner configuration and split ring resonators (SRR) for dielectric characterization of liquids", *IEEE Sensors J.*, vol. 17, pp. 6589-6598, Oct. 2017
[21] M. H. Zarifi, M. Fayaz, J. Goldthorp, M. Abdolrazzaghi, Z. Hashisho, and M. Daneshmand, "Microbead-assisted high resolution microwave planar ring resonator for organic-vapor sensing," *Appl. Phys. Lett*., vol. 106, no. 6, p. 62903, Feb. 2015.
[22] M. Abdolrazzaghi and M. Daneshmand, "Compelling impact of intermodulation products of regenerative active resonators on sensitivity," in *IEEE MTT-S Int. Microw. Symp. Dig*., Jun. 2017, Honolulu (HI), pp. 1018–1021.
[23] M. Abdolrazzaghi and M. Daneshmand, "Dual active resonator for dispersion coefficient measurement of asphaltene nano-particles," *IEEE Sensors J*., vol. 17, no. 22, pp. 7248–7256, Nov. 2017.
[24] M. H. Zarifi et al., "A microwave ring resonator sensor for early detection of breaches in pipeline coatings," *IEEE Trans. Ind. Electron*., vol. 65, no. 2, pp. 1626–1635, Feb. 2018.
[25] M. Abdolrazzaghi, M. H. Zarifi. W. Pedrycz, and M. Daneshmand, "Robust ultra-high resolution microwave planar sensor using fuzzy neural network approach," *IEEE Sensors J*., vol. 17, no. 2, pp. 323–332, Jan. 2017.
[26] F. Martín, F. Falcone, J. Bonache, R. Marqués and M. Sorolla, "Split ring resonator based left handed coplanar waveguide", *Appl. Phys. Lett*., vol. 83, pp. 4652-4654, Dec. 2003.
[27] C. Herrojo, J. Mata-Contreras, F. Paredes, Ferran Martín, "Near-field chipless RFID encoders with sequential bit reading and high data capacity", *IEEE MTT-S Int. Microw. Symp*. (IMS'17), Honolulu, Hawaii, June 2017.
[28] C. Herrojo, J. Mata-Contreras, F. Paredes, F. Martín, "Microwave encoders for chipless RFID and angular velocity sensors based on S-shaped split ring resonators (S-SRRs)", *IEEE Sensors J*., vol. 17, pp. 4805-4813, Aug. 2017.
[29] C. Herrojo, J. Mata-Contreras, F. Paredes, A. Núñez, E. Ramón, F. Martín, "Near-field chipless-RFID tags with sequential bit reading implemented in plastic substrates*", Int. J. Magnetism. Magnetic Mat*., vol. 459, pp. 322-327, 2018.
[30] C. Herrojo, J. Mata-Contreras, F. Paredes, F. Martín, "High data density and capacity in chipless radiofrequency identification (chipless-RFID) tags based on double-chains of S-shaped split ring resonators (S-SRRs)", *EPJ Appl. Metamat*., vol. 4, article 8, 6 pages, Oct. 2017.
[31] C. Herrojo, J. Mata-Contreras, F. Paredes, Ferran Martín, "Near-field chipless RFID system with high data capacity for security and authentication applications*", IEEE Trans. Microw. Theory Techn*., vol. 65 (12), pp. 5298-5308, Dec. 2017.
[32] C. Herrojo, J. Mata-Contreras, F. Paredes, A. Núñez, E. Ramon, and F. Martín "Near-field chipless-RFID system with erasable/programmable 40-bit tags inkjet printed on paper substrates", *IEEE Microw. Wireless Compon. Lett.*, vol. 28, pp. 272- 274, Mar. 2018.
[33] C. Herrojo, J. Mata-Contreras, F. Paredes, A. Núñez, E. Ramon, and F. Martín, "Very Low-Cost 80-Bit Chipless-RFID Tags Inkjet Printed on Ordinary Paper," *Technologies*, vol. 6, no. 2, p. 52, May 2018.
[34] C. Herrojo, F. Paredes, J. Mata-Contreras, E. Ramon, A. Núñez, F. Martín, "Time-domain signature barcodes: near-field chipless-RFID systems with high data capacity", *IEEE Microwave Magazine*, to be published.

Cristian Herrojo was born in Barcelona, Spain, in 1983. He received the Telecommunications Technical Engineering degree in electronic systems and Telecommunications Engineering degree from the Universitat Autònoma de Barcelona in 2010 and 2012, respectively and the PhD degree in Electronics Engineering from the same university in 2018. His research interests include RF/microwave devices, Chipless-RFID and RFID technology, and Metamaterials.
He has authored or co-authored over 12 journal papers and 10 conference papers. He has also filed one patent on Chipless-RFID.

Francisco Javier Muela, was born in Formentera, Spain in 1988. He is studying Telecommunications Technical Engineering degree in Electronic Systems at Universitat Autonoma de Barcelona, and he will present the Bachelor Thesis on September 2018.

Javier Mata-Contreras was born in 1976 in Málaga (Spain). He received the Ingeniería de Telecomunicación Degree from the Universidad de Málaga (UMA) in 2000 and the PhD degree from the same university in 2010, with the Thesis "Distributed Amplifiers and Mixers with Transmission Lines based on Metamaterials". In 2000, he joined the UMA Department of Ingeniería de Comunicaciones UMA as Assistant Professor. He is currently working at CIMITEC and the Universitat Autònoma de Barcelona as Visitant Professor. His research interests include active and passive microwave devices and active distributed circuits based on metamaterials, among others.

Ferran Paredes was born in Badalona (Barcelona), Spain in 1983. He received the Telecommunications Engineering Diploma (specializing in Electronics) and the Telecommunications Engineering degree from the Universitat Autònoma de Barcelona in 2004 and 2006, respectively and the PhD degree in Electronics Engineering from the same university in 2012. He was Assistant Professor from 2006 to 2008 at the Universitat Autònoma de Barcelona, where he is currently working as a Research Assistant. His research interests include metamaterial concepts, passive microwaves devices, antennas and RFID.

Ferran Martín (M'04-SM'08-F'12) was born in Barakaldo, Spain, in 1965. He received the B.S. degree in physics and Ph.D. degree from the Universitat Autònoma de Barcelona (UAB), Barcelona, Spain, in 1988 and 1992, respectively. From 1994 to 2006 he was Associate Professor in Electronics at the Departament d'Enginyeria Electrònica (Universitat Autònoma de Barcelona), and since 2007 he is Full Professor of Electronics. His research activity has been very broad, including the modelling and simulation of electron devices for high frequency applications, millimeter wave and THz generation systems, the application of electromagnetic bandgaps to microwave and millimeter wave circuits, and the application of metamaterial concepts to the miniaturization and optimization of microwave circuits and antennas. He is now very active in the development of microwave sensors for dielectric characterization and motion control, and also in the topic of chipless-RFID. He is the head of the Microwave Engineering, Metamaterials and Antennas Group (GEMMA Group) at UAB, and director of CIMITEC, a research Center on Metamaterials supported by TECNIO (Generalitat de Catalunya). He has organized several international events related to metamaterials, including Workshops at the IEEE International Microwave Symposium (years 2005 and 2007) and European

Microwave Conference (years 2009, 2015, 2017, and 2018), and the Fifth International Congress on Advanced Electromagnetic Materials in Microwaves and Optics (Metamaterials 2011), where he has acted as chair of the Local Organizing Committee. He has acted as Guest Editor in several Special Issues, mainly related to Metamaterials, in various International Journals. He has authored and co-authored over 580 technical conference, letter, journal papers and book chapters, he is co-author of the book on Metamaterials entitled *Metamaterials with Negative Parameters: Theory, Design and Microwave Applications* (John Wiley & Sons Inc. 2008), author of the book *Artificial Transmission Lines for RF and Microwave Applications* (John Wiley & Sons Inc. 2015), co-editor of the book *Balanced Microwave filters* (John Wiley & Sons Inc. and IEEE-Press 2018), and he has generated 19 PhDs. Ferran Martín has filed several patents on metamaterials and has headed several Development Contracts.

Prof. Martín is a member of the IEEE Microwave Theory and Techniques Society (IEEE MTT-S). He is reviewer of the IEEE Transactions on Microwave Theory and Techniques and IEEE Microwave and Wireless Components Letters, among many other journals, and he serves as member of the Editorial Board of IET Microwaves, Antennas and Propagation and International Journal of RF and Microwave Computer-Aided Engineering. He is also a member of the Technical Committees of the European Microwave Conference (EuMC) and International Congress on Advanced Electromagnetic Materials in Microwaves and Optics (Metamaterials). Among his distinctions, Ferran Martín has received the 2006 Duran Farell Prize for Technological Research, he holds the *Parc de Recerca UAB – Santander* Technology Transfer Chair, and he has been the recipient of two ICREA ACADEMIA Awards (calls 2008 and 2013). He is Fellow of the IEEE since 2012 and Fellow of the IET since 2016.